Continuous and Discrete Space Particle Filters for Predictions in Acoustic Positioning

Will Bauer, Surrey Kim, and Michael A. Kouritzin

MITACS-PINTS,
Department of Mathematical and Statistical Sciences, University of Alberta,
Edmonton, Canada, T6G 2G1

ABSTRACT

Predicting the future state of a random dynamic signal based on corrupted, distorted, and partial observations is vital for proper real-time control of a system that includes time delay. Motivated by problems from Acoustic Positioning Research Inc., we consider the continual automated illumination of an object moving within a bounded domain, which requires object location prediction due to inherent mechanical and physical time lags associated with robotic lighting. Quality computational predictions demand high fidelity models for the coupled moving object signal and observation equipment pair. In our current problem, the signal represents the vector position, orientation, and velocity of a stage performer. Acoustic observations are formed by timing ultrasonic waves traveling from four perimeter speakers to a microphone attached to the performer. The goal is to schedule lighting movements that are coordinated with the performer by anticipating his/her future position based upon these observations using filtering theory.

Particle system based methods have experienced rapid development and have become an essential technique of contemporary filtering strategies. Hitherto, researchers have largely focused on continuous state particle filters, ranging from traditional weighted particle filters to adaptive refining particle filters, readily able to perform path-space estimation and prediction. Herein, we compare the performance of a state-of-the-art refining particle filter to that of a novel discrete-space particle filter on the acoustic positioning problem. By discrete space particle filter we mean a Markov chain that counts particles in discretized cells of the signal state space in order to form an approximated unnormalized distribution of the signal state. For both filters mentioned above, we will examine issues like the mean time to localize a signal, the fidelity of filter estimates at various signal to noise ratios, computational costs, and the effect of signal fading; furthermore, we will provide visual demonstrations of filter performance.

Keywords: target tracking, particle system, nonlinear filtering, prediction, acoustic positioning

1. INTRODUCTION

Tracking systems for real-time media control have existed for a number of years. Initially, these systems centered about so-called "Virtual Reality" creation where movements within a small area of perhaps 3m x 3m, were tracked and used to change point of view within computer-modelled 3D worlds. Video images of these worlds were displayed via either video projector or head-mounted video display panels. These images changed in real-time in response to the person's position and angular orientation - a total of six degrees of freedom (three spatial axes plus three rotational angles). An alternate direction of media control exploration has recently arisen in which wireless 3D tracking over areas of large extent (up to 20m x 20m) is used by performers or interactive

Further author information: (Send correspondence to S.K.)
S.K.: E-mail: surrey@math.ualberta.ca
W.B.: E-mail: apr.inc@shawbiz.ca
M.A.K.: E-mail: mkouritz@math.ualberta.ca
PINTS web page: http://www.math.ualberta.ca/pints
A.P.R inc. web page : http://www.positioning-research.com

Image Reconstruction from Incomplete Data II, Philip J. Bones, Michael A. Fiddy, Rick P. Millane,
Editors, Proceedings of SPIE Vol. 4792 (2002) © 2002 SPIE · 0277-786X/02/$15.00

environment participants. In these applications, only 3D (X, Y, Z) coordinates have the potential of being observed in the presence of sensor noise; no angular orientations are directly measured.

A filtering algorithm is used to "clean up" the corrupted measurements of the observed variables and to estimate the components of the performers state that can not be measured, such as the orientation and forward speed. These positional estimates, possibly detailed enough to include gestures, are used to control a variety of media in real-time. The media consist of robotic lights, multi-channel sound systems, and real-time video projections of computer generated images. APR's 3D tracking and media control products are at the forefront of this exploration and their functioning is enhanced by real-time techniques of 3D position prediction. Because of inherent mechanical and physical lags of the different media, real-time tracking for a performer is actually a real-time prediction problem. In this paper we compare two different filtering methods on the acoustic problem, namely the hybrid particle based filter and a Markov chain motivated discrete space filter. Modern filtering theory involves smoothing, tracking, and predicting a signal, like our performer's state, based upon a sequence of distorted, corrupted measurements of part of the signal state. Below, these observations will be comprised of noisy distance measurements from perimeter speakers to the performer.

1.1. Background

We use the reference probability method to describe the solution to this filtering problem in terms of a discrete–time version of the Duncan–Mortensen–Zakai equation and then use particle Markov chain approximations to produce implementable approximate solutions. The later approximations incorporate discretizations of both space and amplitude directly into the unnormalized conditional distribution of the signal given the back observations. Both approximations converge to the actual filtering conditional distribution as the number of particles (and cells in the Markov chain case) increases.

Suppose the signal is described by an *Itô* stochastic differential equation (SDE) defined on some probability space $(\Omega, \mathcal{F}, \mathbf{P})$, and living within a d-dimensional rectangular domain $D = [0, L_1] \times [0, L_2] \times \cdots \times [0, L_d]$, where $L_i, 1 \leq i \leq d$ are the lengths of all dimensions. A general stochastic signal motion model is defined by

$$\begin{cases} dx_t = b(x_t)dt + g(x_t)dv_t \\ x_0 = x \ , \end{cases} \tag{1}$$

where x_t is the signal state at time t and v_t is a standard d-dimensional Brownian motion. We assume that b and g have been chosen in a manner to ensure that x_t stays in D. Let $a(x) = g(x)g^*(x)$ be the diffusion matrix. The diffusion operator $(L, \mathcal{D}(\mathcal{L}))$ for the stochastic equation defined above is

$$L = \frac{1}{2} \sum_{i,j=1}^{d} a_{i,j}(x) \frac{\partial^2}{\partial x_i \partial x_j} + \sum_{j=1}^{d} b(x) \frac{\partial}{\partial x_j} \tag{2}$$

and the associated adjoint operator is given by

$$L^* = \frac{1}{2} \sum_{i,j=1}^{d} a_{i,j}(x) \frac{\partial^2}{\partial x_i \partial x_j} + \sum_{j=1}^{d} \tau_j(x) \frac{\partial}{\partial x_j} + \nu(x) \tag{3}$$

where $\tau_j(x) = \sum_{i=1}^{d} \frac{\partial a_{i,j}(x)}{\partial x_i} - b_j(x)$ and $\nu(x) = \frac{1}{2} \sum_{i,j=1}^{d} \frac{\partial^2 a_{i,j}(x)}{\partial x_i \partial x_j} - \sum_{j=1}^{d} \frac{\partial b_j(x)}{\partial x_j}$.
Let $\varepsilon > 0$; set $t_m := m\varepsilon$ for $m = 1, 2, \ldots$; take h to be the sensor function, and let W be a standard $\mathbb{R}$-valued Brownian motion independent of $\{x_t\}$. For $h \in C(D)$, we then define

$$Y_{t_m} = h(x_{t_m})\Delta t_m + \sigma \Delta W_{t_m} \tag{4}$$

to be a noisy observation sequence of the signal x_{t_m} at times t_m with $\Delta W_{t_m} = W_{t_m} - W_{t_{m-1}}$, and define $\mathcal{Y}_t \doteq \sigma\{Y_{t_m}, t_m \leq t\}$ to be the information observed up to time t.
For all real measurable functions f on D such that $\mathbf{E}|f(x_t)|^2 < \infty$ for all $0 \leq t \leq T$, the filtering problem is to evaluate

$$\pi_t(f) := \mathbf{E}[f(x_t)|\mathcal{Y}_t], \quad t \in [0, T], \tag{5}$$

which is the least square estimate of $f(x_t)$ given all the discrete observations up to time t. For each Borel function f and $t \in [0,T]$, we call any version of $\pi_t(f)$ in equation (5) an optimal filter. We define

$$\zeta_m := \exp\{h(x)\frac{Y_{t_m}}{\sigma^2} - \frac{\varepsilon}{2\sigma^2}h^2(x)\} \tag{6}$$

and

$$\overline{\zeta}_m = \zeta_m - 1. \tag{7}$$

Using the convention that the product over zero elements is 1, we set $\eta_t := \Pi_{m=1}^{\lfloor t/\varepsilon \rfloor}\zeta_m(x_{t_m})$. Hereafter, $\lfloor r \rfloor$ denotes the greatest integer not more than a real number r. We define a probability measure $\mathbf{P}^0$ on $(\Omega, \mathcal{F})$ by $d\mathbf{P}^0/d\mathbf{P} := \eta_T^{-1}$ and let $\mathbf{E}^0$ denote the expectation with respect to $\mathbf{P}^0$. Under $\mathbf{P}^0$ the distribution of $\{x_t\}$ is the same as under $\mathbf{P}$ and $\{Y_{t_m},\ m = 1, 2, \dots\}$ is a sequence of Gaussian random variables independent of $\{x_t\}$ with mean zero and variance $\sigma^2\varepsilon$. Then, one has the Kallianpur-Striebel formula

$$\pi_t(f) = \frac{\mathbf{E}^0[f(x_t)\eta_t|\mathcal{Y}_t]}{\mathbf{E}^0[\eta_t|\mathcal{Y}_t]} := \frac{\overline{p}_t^y(f)}{\overline{p}_t^y(1)}. \tag{8}$$

For any $f \in \mathcal{D}(\mathcal{L})$, we find, from integration by parts and independence, that

$$\overline{p}_t^y(f) = \overline{p}_0^y(f) + \int_0^t \overline{p}_s^y(\mathcal{L}f)ds + \sum_{m=1}^{\lfloor t/\varepsilon \rfloor} \mathbf{E}^0[f(x_{t_m-})\eta_{t_m-}\overline{\zeta}_m(x_{t_m})|\mathcal{Y}_t], \qquad a.s.\ \mathbf{P}^0. \tag{9}$$

Under ellipticity and smoothness condition on a,b, one finds that $\overline{p}_t^y$ has a density $p(t,x)$ on $(H, \langle\cdot\rangle_H) := L^2(D;dx)$, which is the path-wise unique solution to the random integral equation on H

$$\langle p_t, f\rangle_H = \langle p_0, f\rangle_H + \int_0^t \langle p_s, \mathcal{L}f\rangle_H ds + \sum_{m=1}^{\lfloor t/\varepsilon \rfloor} \langle p_{t_m-}, \overline{\zeta}_m f\rangle_H, \qquad \forall f \in \mathcal{D}(\mathcal{L}),\ t > 0,\ x \in D, \tag{10}$$

where $p(0,x) = p_0(x)$ for $x \in D$, and the density function p_0 of the distribution of x_0 is assumed to be in H.

1.2. Particle Filters

Particle-based nonlinear filters are effective and versatile methods for computing approximations to filtering problems. The basic requirements for a particle method are simulation of particles with the same law as the signal and the re-sampling of these particles to incorporate observation information effectively. Then, the high-particle limit of an empirical measure for the resulting particle system can be anticipated to exist and yield the conditional distribution of the signal at a particular time given the back observations. The *weighted-interacting* hybrid particle method is thought to possess an excellent compromise between the unadaptive nature of the weighted particle method and the overly random resampling in classical interactive particle methods; furthermore, this method accepts the extent of resampling as a problem dependent parameter ρ. A particle in the hybrid method simply runs as a weighted particle until such time as its weight differs significantly from the majority of the particle weights. In particular, after every observation a particle with a weight at least ρ times larger than another is combined with the low weighted particle. The low weighted particle is moved to the higher weighted particle's site with a high probability and, otherwise, the high weighted particle is moved to the low one's site. In either case, the weights of both particles are reset to the average of the two original particle weights. This process starts from the highest weighted particles in the system to the lowest. The resampling is valid since the two particles, after recombination, being either at the site of the precombination lower or higher weighted particle, have the same expected weight as before. This recombination procedure is repeated until all weights are within ρ of each other, and then the conditional distribution approximations for particle ξ^j with weight $\widetilde{W}_m$ after the mth observation are

$$P\left(X_{t_m} \in A | Y_{t_1}, \dots, Y_{t_m}\right) \approx \frac{1}{\sum_{j=1}^{M_{t_m}} \widetilde{W}_m(\xi^j)} \sum_{j=1}^{M_{t_m}} \widetilde{W}_m(\xi^j) 1_{\xi_{t_m}^j \in A}\,. \tag{11}$$

where M_{t_m} is the total number of particles at time t_m. Equation (11) is a direct approximation to (equations 5 & 8).

In the aforementioned adaptive weighted particle method each particle is simulated independently according to the law of the signal between observations. In particular, when the signal has a continuous state space, as in the problem of current interest, so do the particles. All resampling calculations are done on a particle-by-particle basis regardless of whether other nearby particles require entirely similar calculations. An alternative approach is to group nearby particles into cells. This group treatment not only requires less extensive computer resources but also reduces unwanted resampling noise. Ideally, the discrete space particle system would be constructed to achieve the correct inter-cell flows and observation-dependent resampling with a minimal amount of calculation and resampling noise. Below and in a later section we describe such a system that has already been shown[5] to perform very well. Our discrete-space particle system is constructed by discretizing our basic filtering equation (10) directly (as opposed to discretizing the signal in more classical works) and then applying Poisson process time change techniques. In particular, we assume a density for the conditional distribution of the signal given the back observations and approximate this density via

$$\widehat{p}^N(t,x) = \sum_{k \in D_N} n_k^N(t) 1_k^N(x) / \sum_{k \in D_N} n_k^N(t) \,, \tag{12}$$

where $n_k^N(t)$ is the number of particles in cell k at time t. Equation (10) is used to derive an initial equation for n_k^N and time-change techniques are then used to turn n_k^N into a Markov chain. We carefully reduce rates by subtracting in and out flows to yield an efficient birth-death only Markov chain technique. The net benefit of all our rate reduction is a typically fast, accurate approximation. In contrast to the hybrid method approximation to Equations (8) & (9) (see Equation (11) above), the discrete space filter does not store weights for each particle or even distinguish between "nearby" particles, but rather bases its particle count adjustment decisions on all particles in cells. The conditional distribution approximation in a discrete space filter is calculated by

$$P\left(X_{t_m} \in A \middle| Y_{t_1}, \ldots, Y_{t_m}\right) \approx \frac{1}{M_{t_m}} n_k^N(t_k) 1_{k \in A}. \tag{13}$$

where M_{t_m} is the total number of particles at time t_m, and $n_k^N(t)$ is the number of particles in cell k at time t_m.

The algorithm to implement our filter is reduced to an algorithm to implement a specific time–inhomogeneous Markov chain, which can be done using a single Poisson process and independent sequences of Bernoulli trials. The inhomogeneity is due to the observations themselves. The discretization of amplitude results in *particles* representing a small mass of the conditional distribution at particular grid points in the signal domain. These particles diffuse, drift, give birth, and die within the region similarly to those of continuous–state particle filters except we do not distinguish between particles in a cell and only worry about net flow of particles. The particle locations include information from the observations through observation–dependent births and deaths.

2. PERFORMER TRACKING PROBLEM

APR Inc.'s wide-area 3D tracking and media control products track performers or interactive environment participants as they move within areas of large extent (up to 20m x 20m). Performers are tracked in 3D via a small ultrasonic microphone (typically carried in hand or worn on the shoulder or head) which senses pulses emitted by four ultrasonic speakers arranged around the perimeter of the tracking area. Lag times resulting from having to track over areas of large extent and from the mechanical delays inherent in devices such as robotic lighting require predictive calculations to enhance the quality of media responsiveness to gestural data. This problem is particularly acute in the case of robotic lighting "follow-spot" behavior where lights track participants as they move around within an interactive space. Combined time lags can range up to half a second depending on tracking area and light mechanics. Additionally, once the participant is initially found by the system, the system must be robust in that it be able to function in the presence of signal "fading" due to occlusion of tracking transducers by the participant, other humans present, or theater props contained within the interactive space.

Traditionally, Kalman filters have been used to provide estimates of performer position at future times, allowing lights to "lead" the performer as he/she moves about. This research was engendered as a result of APR's dissatisfaction with Kalman filters. They are problematic for a number of reasons: there are practical problems such as matrix instability and brittleness; setting Kalman matrix coefficients can be a matter of some trial and much error; there is normally no incorporation of additional information gained from the use of performer motion models; and finally, there is considerable difficulty in extending Kalman filters to more complex representations of system functionality as embodied in performer motion models and tracking system observation models.

Below we give a nonlinear motion model for the performer as well as a nonlinear observation model, both unsuitable for the Kalman filter, and develop nonlinear filtering algorithms to predict future performer position based upon real observation data.

2.1. Performer Motion Model

In modeling our performer's motion, there are considerations in constructing the drift and diffusion coefficients, denoted $b(X_t)$ and $g(X_t)$ respectively in equation (1), to mimic not only a realistic performer on stage but also a general one. The performer's state is a bounded 5-dimensional real-valued vector (x, y, z, f, θ) where (x, y, z) is the vector position of the performer with center stage floor being the origin $(0, 0, 0)$. For simplicity, we describe only the forward speed as $f_{min} \leq f \leq f_{max}$ allowing the performer to walk backwards when $f_{min} < 0$. The orientation of the performer is labeled θ, where $\theta = 0$ $rads$ when the performer is facing the audience. The mathematical model for the performer's motion is described in equation (14) below. Evolution for the x and y position is dependent on both the current forward speed and orientation. Equations for both the z position and speed f are, in fact, $Itô$ SDEs. The drifts are towards a constant parameter $\frac{2z_{max}+z_{min}}{3}$ and f_{avg}, which correspond respectively to the height placement of a microphone on a performer, and to a natural stage performer's walking speed. Randomness in z and f are "turned off" at the lower and upper bounds by the diffusive part of the equation. The square root function, versus a linear one, is used to ensure the noise is turned off slowly. Modeling for the performer's orientation involves considerations in simple stage concepts such as a drift to face an audience and a pull back to the center stage when near the ends. Because of the periodic nature of $-\pi < \theta \leq \pi$ the model was first designed as a 2-dimensional diffusion on a circle. Then, converting back to a scalar $Itô$ formula, we have the equation for θ (see below equation 14), which is good for $\theta \in (-\pi, \pi)$. For simplicity reasons, we omit the mathematical description involving local time for $\theta \in (-\pi, \pi]$ and merely mention that we force periodic boundary conditions such that θ lives in the interval $(-\pi, \pi]$ by "resetting" $\theta \in R$ to the equivalent angle in $(-\pi, \pi]$
The complete model is given below

$$
\begin{aligned}
dx_t &= f_t \cos(\theta_t)dt \\
dy_t &= f_t \sin(\theta_t)dt \\
dz_t &= \alpha_z(\frac{2z_{max} + z_{min}}{3} - z_t)dt + \sigma_z\sqrt{(z_{max} - z_t)(z_t - z_{min})}dB_t^z \\
df_t &= \alpha_f(f_{avg} - f_t)dt + \sigma_f\sqrt{(f_{max} - f_t)(f_t - f_{min})}dB_t^f \\
d\theta_t &= \Big(-\alpha_{\theta_1}\theta_t - \alpha_{\theta_2}\Lambda(X_t)\sqrt{(\cos(\theta_t) + \frac{x_t}{\sqrt{x_t^2 + y_t^2}})^2 + (\sin(\theta_t) + \frac{y_t}{\sqrt{x_t^2 + y_t^2}})^2}\Big)dt + \sigma_\theta dB_t^\theta
\end{aligned}
\tag{14}
$$

where B_t^z, B_t^f and B_t^θ are independent standard Brownian motions, and

$$
\Lambda(X_t) = \begin{cases} if(\arctan(x_t, y_t) \leq 0) \begin{cases} -1 & \arctan(x_t, y_t) < \theta_t \leq \arctan(x_t, y_t) + \pi \\ 1 & otherwise \end{cases} \\ \\ if(\arctan(x_t, y_t) > 0) \begin{cases} 1 & \arctan(x_t, y_t) - \pi < \theta_t \leq \arctan(x_t, y_t) \\ -1 & otherwise \end{cases} \end{cases}
$$

describes which direction the performer will turn. $\Lambda(X_t) = -1$ signifies a drift in a counter clock-wise direction. Some constant performer parameters that are used for our simulation runs are given in the table below.

Performer Parameters	Value	Performer Parameters	Value
z_{min}	0.0	f_{min}	-0.4
z_{max}	1.0	f_{avg}	1.5
σ_z	0.15	f_{max}	2.9
α_z	0.9	σ_f	0.75
σ_θ	0.5	α_f	0.75
α_{θ_1}	0.2		
α_{θ_2}	0.4		

2.2. Acoustic Observation Model

Modeling of the ultrasonic tracking process must be based on the physical functionality of the tracking system itself. APR's 3D ultrasonic tracking technology involves four speakers which are placed in an approximate rectangle around the perimeter of the desired interactive area. The speakers are calibrated so that their 3D position (X, Y, Z) coordinates are known relative to a user-defined frame of reference in the center of the interactive area. The speakers emit ultrasonic pulses with a duration of about 1 millisecond at a frequency around 20 kHz. Firing of the four speakers is time multiplexed with each speaker waiting long enough for a pulse to clear the interactive area before another speaker is fired. These pulses arrive at the ultrasonic microphone carried by a performer and are radio telemetered back to a PC computer where they are digitized and processed by a DSP chip to extract their timing information i.e. the elapsed "time of flight" between when the pulse was emitted and when it was received at the microphone. There is an appreciable but fixed delay introduced by the telemetry and digitization process. Noise is superimposed upon this signal due to phasing of the ultrasonic carrier frequency with the digitization rate plus the fading of signals due to the presence of low level pulse reflections from previous pulses which are still bouncing about the tracking area. These reflections, while not of high enough amplitude to be counted as pulses, affect the rise-time of the current ultrasonic pulse's arrival via phase cancellation. The reflections, of course, change in relation to room position and the positions of people/objects within the room. While in theory it is possible to model these reflections, it is not practically possible to gather enough information about room geometry and wall surface composition to do so. Furthermore, the chance of a very poor reading increases as the performer's orientation tends away from a particular speaker, with the poorest chance of a valid reading when the performer's back intrudes between the speaker's line of fire and the microphone. We have found it possible to treat the errors as random Gaussian noise, with an orientation dependent probability of missed observations. The distance measurements between one of four speakers and the performer's ultrasonic microphone is given by the sensor function

$$h(X_{t_m}, S^l) = \sqrt{\left((S_x^l - x)^2 + (S_y^l - y)^2 + (S_z^l - z)^2\right)} \tag{15}$$

where $l = \{0, 1, 2, 3\}$ is an integer index for the four speakers. Typically these radial position measurements are accurate to within about ± 10 cm. To further contrast differences between our two test filters, our simulations are run with a range of observation noises. An observation at time t_m is either constructed by adding zero-mean independent Gaussian random variable $\{\Delta W_{t_m},\ m = 1, 2, \cdots\}$ where W is a standard $\mathbb{R}$-valued Brownian motion, or declared invalid according to the formula

$$Y_{t_m} = \begin{cases} h(X_{t_m}, S^l) + \sigma \Delta W_{t_m} & , if \quad U_m(0,1) < p \\ -1 & , otherwise \end{cases} \tag{16}$$

where $l = m \mod 4$ represents the last speaker number fired, $\{U_m(0,1),\ m = 1, 2, \cdots\}$ is an independent sequence of $[0,1]$-Uniform random variable, and $p = 0.97 - 0.67\frac{|\phi|}{\pi}$ is the probability of a valid observation reading with ϕ being the angle between the performer orientation and speaker l.

2.3. Stage Model

The tracking area of the performer's stage is constrained by our four perimeter speakers, and has dimensions 10.0m x 10.0m x 7.0m. With center stage being (0,0,0), the four speakers' coordinates used in equation (15) are

Stage Parameters	S_x	S_y	S_z
S^0	-5.0	-5.0	7.0
S^1	-5.0	5.0	7.0
S^2	5.0	-5.0	7.0
S^3	5.0	5.0	7.0

2.4. Objective

The problem is to estimate the conditional distribution of the performer's 3 dimensional position, κ time units into the future, based on the noisy back observations.

$$P(X_{t_m+\kappa} \in dx | \sigma\{Y_{t_q}, 0 \le q \le m\}). \tag{17}$$

3. FILTER TECHNIQUES

Considerations such as the data structure used greatly affect both hybrid and discrete space filter fidelity and efficiency. Although the implementations for the two methods have important computer science component we do not clutter the descriptions of the algorithms with all practical programming efficiencies. Simulations were developed and run on a DEC-ALPHA UP1500 833 MHz system.

3.1. Hybrid Update Algorithm

The basic refining hybrid algorithm proceeds as follows:

1. Initialize particles $\{\xi_0^1, \xi_0^2, \ldots, \xi_0^M\}$ uniformly over the domain $[0, L_1] \times [0, L_2] \times \cdots \times [0, L_d]$, thus yielding $\frac{1}{M}\sum_{j=1}^{M} \delta_{\xi_t^j}$ as a good approximation to the assumed uniform distribution of X_0. Set $\widetilde{W}_0(\xi^j) = 1$, $\forall j = 1, \ldots, M$.

2. Repeat for $m = 1, 2, \ldots$

   (a) Evolve all particles over time interval ϵ using, for example, Euler approximations. Call the new particles just prior to an observation $\left\{\xi_{t_{m-}}^1, \xi_{t_{m-}}^2, \ldots, \xi_{t_{m-}}^M\right\}$.

   (b) Upon receiving the m^{th} observation, Y_{t_m}, calculate the weight for all $\left\{\xi_{t_{m-}}^1, \xi_{t_{m-}}^2, \ldots, \xi_{t_{m-}}^M\right\}$ according to $\widetilde{W}_m(\xi^j) = W_m(\xi^j)\widetilde{W}_{m-1}(\xi^j)$, where $W_m(\xi^j) = \exp\{\frac{h(\xi_{t_m}^j)Y_{t_m} - \frac{\epsilon}{2}h^2(\xi_{t_m}^j)}{\sigma^2}\}$.

   (c) Resample two particles at a time ξ^i and ξ^j while $\widetilde{W}_m(\xi^i) < \rho\widetilde{W}_m(\xi^j)$, $\forall i, j = 1, \ldots, M$..

   (d) Relabel the resulting particles $\{\xi_{t_m}^1, \xi_{t_m}^2, \ldots, \xi_{t_m}^M\}$.

   (e) The conditional distribution for the signal location is approximated by

   $$P\left(X_{t_m} \in A | Y_{t_1}, \ldots, Y_{t_m}\right) \approx \frac{1}{\sum_{j=1}^{M} \widetilde{W}_m(\xi^j)} \sum_{j=1}^{M} \widetilde{W}_m(\xi^j) 1_{\xi_{t_m}^j \in A}$$

   .

   (f) Predictions are then made for $t_m + \kappa$ by evolving all the particles over the time κ to yield the conditional estimate for equation (17)

   (g) The empirical estimate for the signal is calculated as the conditional expectation

   $$E[X_{t_m} | \, Y_{t_l}, 1 \le l \le m] \approx \frac{1}{\sum_{j=1}^{M} \widetilde{W}_m(\xi^j)} \sum_{j=1}^{M} \widetilde{W}_m(\xi^j)\xi_{t_m}^j.$$

3.2. Discrete Space Update Algorithm

The Markov chain approximation discussed in this paper is motivated by the stochastic particle models of chemical reaction with diffusion. We first define the mesh or grid via a vector of integers $N := (N_1, N_2, N_3, \cdots, N_d)$, where each $N_i \in \mathbb{N}$, we let $D_N := \{k = (k_1, \ldots, k_d) \in \mathbb{N}^d : 1 \leq k_i \leq L_i N_i \text{ for each } 1 \leq i \leq d\}$ and divide $[0, L_1) \times \cdots \times [0, L_d)$ into $L_1 N_1 \times \cdots \times L_d N_d$ cells of size $\frac{1}{N_1 \times N_2 \times \cdots \times N_d}$:

$$I_k^N := \left[\frac{k_1 - 1}{N_1}, \frac{k_1}{N_1}\right) \times \cdots \times \left[\frac{k_d - 1}{N_d}, \frac{k_d}{N_d}\right), \quad k \in D_N. \tag{18}$$

We denote $\nu(x) := \frac{1}{2}\sum_{i,j=1}^{d} \frac{\partial^2 a_{i,j}(x)}{\partial x_i \partial x_j} - \sum_{j=1}^{d} \frac{\partial b_j(x)}{\partial x_j}$. For $k \in D_N$, we define $h_k^N := (N_1 \times N_2 \times \cdots \times N_d) \int_{I_k^N} h(x)dx$, $\nu_k^N := (N_1 \times N_2 \times \cdots \times N_d) \int_{I_k^N} \nu(x)dx$, $\tau_{k,j}^N := (N_1 \times N_2 \times \cdots \times N_d) \int_{I_k^N} \tau_j(x)dx$, and $a_{ij}^N(k) := (N_1 \times N_2 \times \cdots \times N_d) \int_{I_k^N} a_{ij}(x)dx$ for $1 \leq i, j \leq d$.

Now, we let $\{X_{+,N}^{k,y}(t), X_{-,N}^{k,y}(t); X_{+,N}^{k}(t), X_{-,N}^{k}(t); k \in D_N\}$ be independent Poisson processes on some probability space $(\overline{\Omega}, \overline{\mathcal{F}}, \overline{\mathbf{P}})$ for each $N \in \mathbb{N}^d$. We define from $(\Omega, \mathcal{F}, \mathbf{P}^0)$ and $(\overline{\Omega}, \overline{\mathcal{F}}, \overline{\mathbf{P}})$ the product probability space $(\Omega_0, \mathcal{F}_0, \mathbf{P}_0) = (\Omega \times \overline{\Omega}, \mathcal{F} \otimes \overline{\mathcal{F}}, \mathbf{P}^0 \times \overline{\mathbf{P}})$. Let $M_t(N)$ denote the total number of particles at time t and be such that $M_0(N) \to \infty$ as $N \to \infty$ and

$$n_k^N(0) = \left\lfloor M_0(N) \int_{I_k^N} \hat{p}_0(x)dx \right\rfloor. \tag{19}$$

Moreover the "number of particles" in cell k at time t will be denoted by $n_k(t)$. Collectively $\{n_k(t)\}_{k \in D_N}$ form a Markov chain that using time change methods can be described as follows:

$$\begin{aligned}
n_k^N(t) = \quad & n_k^N(0) + X_{+,N}^{k,y}\left(\sum_{m=1}^{\lfloor t/\varepsilon \rfloor}\left[\left\{exp\left(\frac{h_k^N\left(Y_{t_m}\right) - \frac{\varepsilon}{2}\left(h_k^N\right)^2\right)}{\sigma^2_{observation}}\right) - 1\right\} n_k^N(t_{m^-})\right]^+\right) \\
& - X_{-,N}^{k,y}\left(\sum_{m=1}^{\lfloor t/\varepsilon \rfloor}\left[\left\{exp\left(\frac{h_k^N\left(Y_{t_m}\right) - \frac{\varepsilon}{2}\left(h_k^N\right)^2\right)}{\sigma^2_{observation}}\right) - 1\right\} n_k^N(t_{m^-})\right]^-\right) \\
& + X_{+,N}^{k}\left(\int_0^t\left[\sum_{i,j=1}^{d}\frac{1}{2}a_{i,j}^N(k)N_i \times N_j\left[n_{k+e_i}^N(s) - n_k^N(s) - n_{k+e_i-e_j}^N(s) + n_{k-e_j}^N(s)\right]\right]^+ ds\right) \\
& + X_{+,N}^{k}\left(\int_0^t\left[\nu_k^N n_k^N(s) + \sum_{j=1}^{d}\tau_j^N(k)N_j\left(n_{k+e_j}^N(s) - n_k^N(s)\right)\right]^+ ds\right) \\
& - X_{-,N}^{k}\left(\int_0^t\left[\sum_{i,j=1}^{d}\frac{1}{2}a_{i,j}^N(k)N_i \times N_j\left[n_{k+e_i}^N(s) - n_k^N(s) - n_{k+e_i-e_j}^N(s) + n_{k-e_j}^N(s)\right]\right]^- ds\right) \\
& - X_{-,N}^{k}\left(\int_0^t\left[\nu_k^N n_k^N(s) + \sum_{j=1}^{d}\tau_j^N(k)N_j\left(n_{k+e_j}^N(s) - n_k^N(s)\right)\right]^- ds\right) \quad .
\end{aligned} \tag{20}$$

Equation (20) provides a very explicit and powerful construction of a Markov chain used in equation (21) below to approximate equation (8), and can be implemented directly on a computer. The basic construction of the discrete space particle filter proceeds as follow:

1. Initialize the initial $(N_1 \times N_2 \times \cdots \times N_d)$ cells by injecting all $n_k^N(0)$ particles in cell k.
2. Evolve the Markov chain system over the time interval ϵ using the time changed independent Poisson processes as in equation (20).

3. Upon receiving the m^{th} observation, at time t_{m^-} resample using the observation processes described in equation (20).

4. Predictions are then made for $t_k + \kappa$ by evolving the system over the time κ to yield the conditional estimate for equation (17)

To obtain the density in each cell, we divide $n_k^N(t)$ by M_t and consequently the description of the stochastic particle model can be given by

$$\hat{p}^{l,N}(t,x) = \sum_{k \in D_N} \frac{n_k^N(t)}{M_t} 1_k^N(x), \tag{21}$$

where $1_k^N(\cdot)$ denotes the indicator function on I_k^N. In Kouritzin, Long, and Sun,[4] it is shown that similar approximations converge to the actual unnormalized filtering conditional distribution as the discretization mesh is refined. More precisely, the law of large numbers holds for each fixed $\omega \in \Omega$.

4. FILTER COMPARISONS

4.1. The Simulation

A graphical presentation of the simulations have been constructed, as depicted in Fig. 1. This is one frame of an animation that follows the observation sequence. The top left panel indicates the simulated performer position and orientation in red. The top right panel is the 2-dimensional graphical representation of our observation sequence where an arc is the noisy cross-section of the spherical distance between a speaker and microphone. The bottom two panels display a filter's current estimate of the conditional distribution of the signal's position. The hybrid filter is at left and the discrete space filter is at the right. Below the discrete space filter label is a panel with the current N (partition of the dimensions in the following order : partition for x, y, z, f, θ).

4.2. Problem Setup

We run both the refining hybrid and the discrete space filter against a simulated signal-observation model as described above (Sect.2). For our simulations, the total number of particles, M, used in each of the filters, the observation noise, $\sigma_{observation}$ from equation (16), the starting and ending grid size N for the discrete space filter (see Sect. (3.2), and the parameter ρ for the refining hybrid filter (see Sect. (3.1)), are listed in the table below. The total particle count is approximately maintained at the constant M_0 throughout the use of each filter. For the simulations, both filters assume no *a priori* knowledge of the signal state, so that the initial signal density $p_0(x)$ is taken to be uniform. Here are the parameters for the two different acoustic tracking/predicting problem scenarios (labeled A and B). We simulate over a time period of 50 or 100 observation arrivals with valid or invalid (see equation (16)) observations arriving every $\varepsilon = 0.02$ time units. Predictions are made by both filters $\kappa = 0.2$ time units into the future.

Simulation Parameters	Scenario A	Scenario B
Simulated Time Units	1.0	2.0
M_0	5000	5000
$\sigma_{observation}$	0.20	0.40
Discrete Space Filter's Starting $N_0 =$	(8,8,128,4,32)	(4,4,128,4,32)
Discrete Space Filter's Max $N_t =$	(32,32,128,32,32)	(32,32,128,32,32)
Hybrid Filter's ρ	75.0	200.0

For both scenarios we compare the processing time and fidelity in mean square error for both tracking and prediction of our simulated performer (see section (2.1)). For both filters we compute the mean-square error for the position estimates of the performer

$$MSE(t) = d(x_t, \mathbf{E}^n[x_t|\mathcal{Y}^t]) \tag{22}$$

from the estimated distribution of the filters and from the true signal value at the time of each observation. The function d here is Euclidean distance and $\mathbf{E}^n[x_t|\mathcal{Y}^t]$ denotes the approximate empirical conditional expectation of x_t given $\mathcal{Y}^t$ as calculated by either the hybrid or Markov chain algorithm. For calculating the prediction MSE we use the filters' estimates from time t and the true signal value at time $t+\kappa$

$$MSE(t) = d(x_{t+\kappa}, \mathbf{E}^n[x_{t+\kappa}|\mathcal{Y}^t]) \tag{23}$$

The data are averaged over a hundred simulation runs for each problem scenario.

4.3. Comparison Data

Graphs of the average mean square error in the position estimate over the simulated time are provided for the two scenarios (Sect. 4.2), averaged over 100 runs, in figures 2 - 3.

For both problem scenarios the continuous space particle method outperforms the discrete space counterpart in mean square error for both tracking and prediction estimates by approximately 77-80% (see figures (2

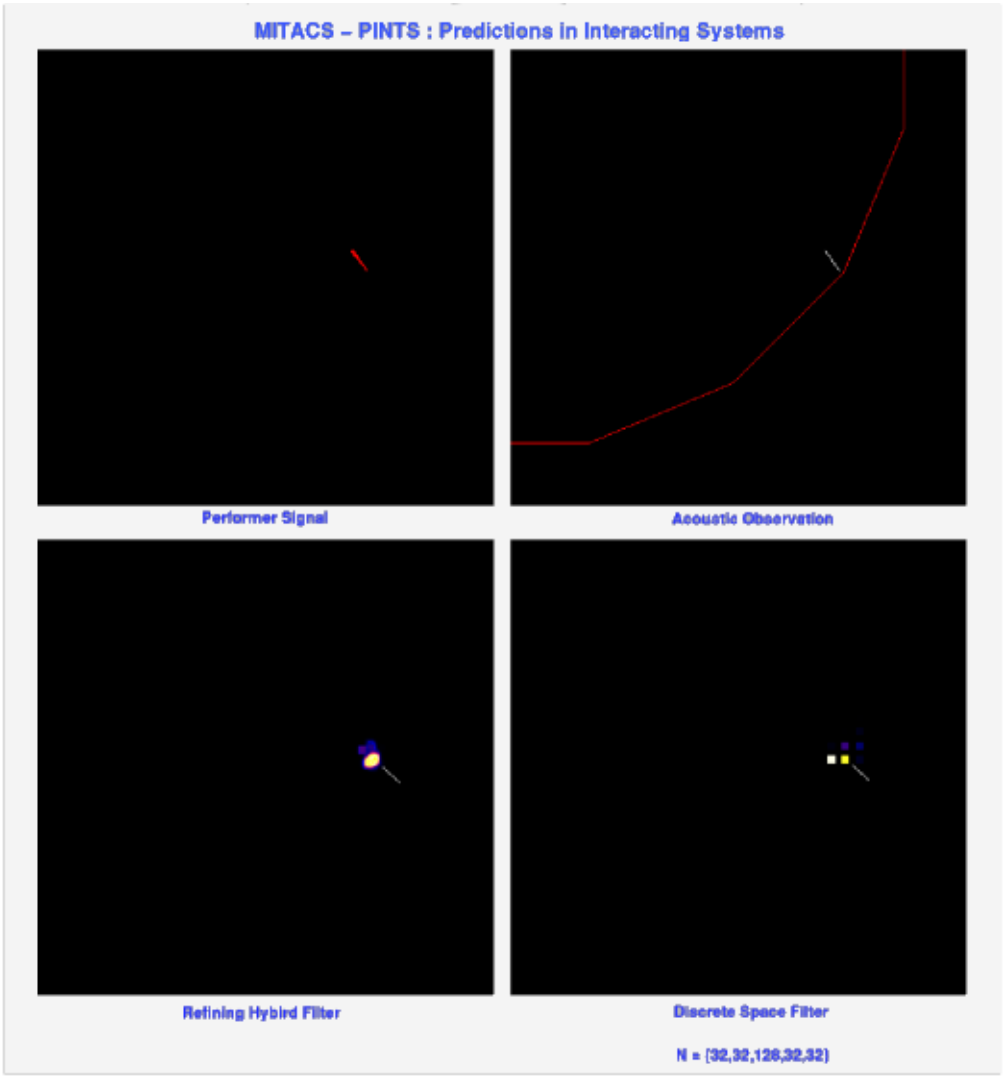

Figure 1. Sample frame from a performer tracking problem animation.

- 3 for graphs of MSE for problem scenario A; similar results follow for problem scenario B). There is an obvious correlation with the error in estimates and the error in predictions; this is expected since we use the most current estimated distribution to construct predictions. The lesser performance of the discrete space filter is because of a constraint on the maximum value for N (see table in Sect.4.2) used in our simulations. The corresponding finest possible grid sizes for each dimension are, in the dimension order x, y, z, f, θ : $0.3125m, 0.3125m, 0.0078125m, 0.103125\frac{m}{s}, 0.19635rads$. The reason for a maximum grid partition is due to limiting computational resources when dealing with a five-dimensional signal state. As mentioned before in section (3), the implementation for the discrete space filter is heavily computer science oriented, and thus may be improved in the future.

Results for computation times in both scenarios (graphs in figures (4 - 5)) on average tend to favor the discrete space filter. The jumps in computation time seen in the graph for problem scenario A occur when the discrete space filter increases a N_i to further "zoom in" on that particular dimension i, $1 \leq i \leq d$. Modifications in the implementation parameters controlling how and when the filter "zooms in" will determine the smoothness in these jumps (see graph for problem scenario B in figure (5) depicting smoother transitions of N). In general, the computation time for resampling in the discrete space method will be less than that of a particle method's individual particle-by-particle treatment, because of the grouping of nearby particles in cells. This effect is accentuated as the number of particles increases. In problem scenario A the discrete space filter is approximately 33% faster then the hybrid filter, and in scenario B approximately 66% faster.

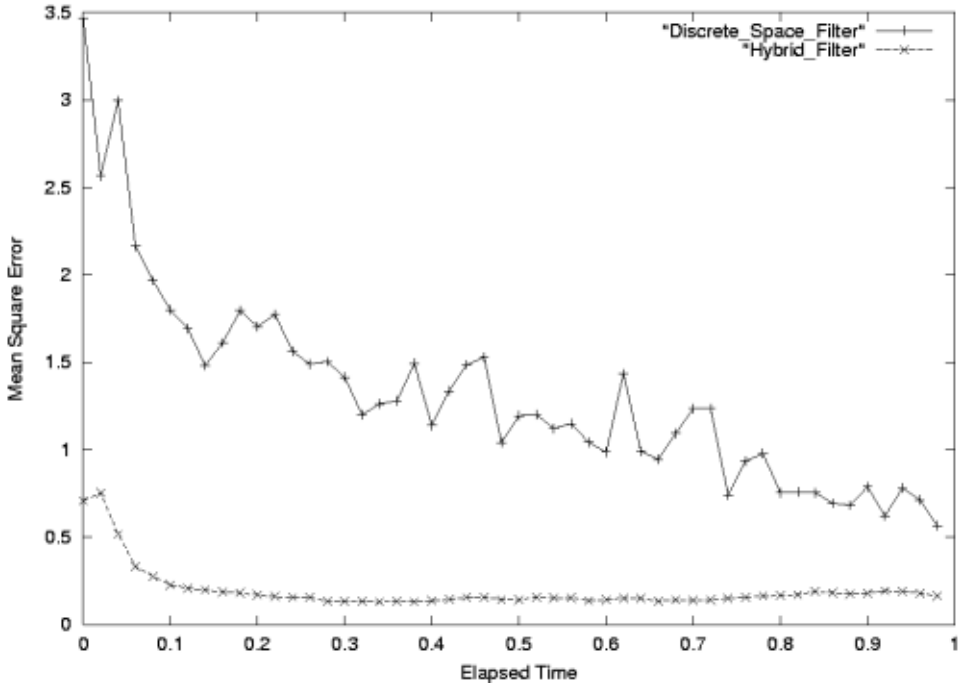

Figure 2. Average mean square error in performer's state estimate for Scenario A.

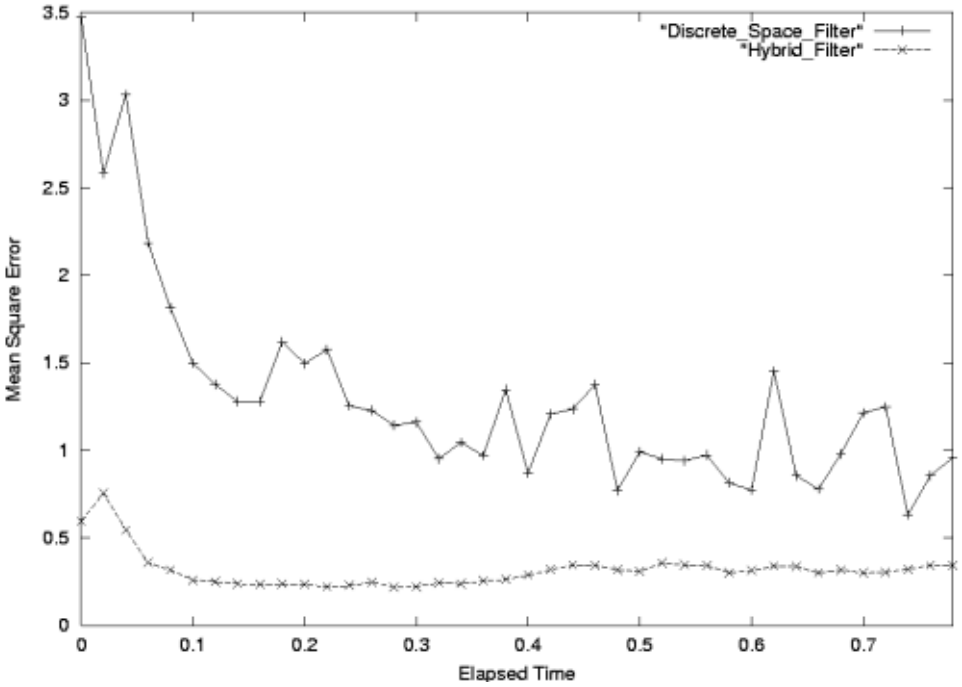

Figure 3. Average mean square error in prediction ($\kappa = 0.2$ time units) of performer's state for Scenario A.

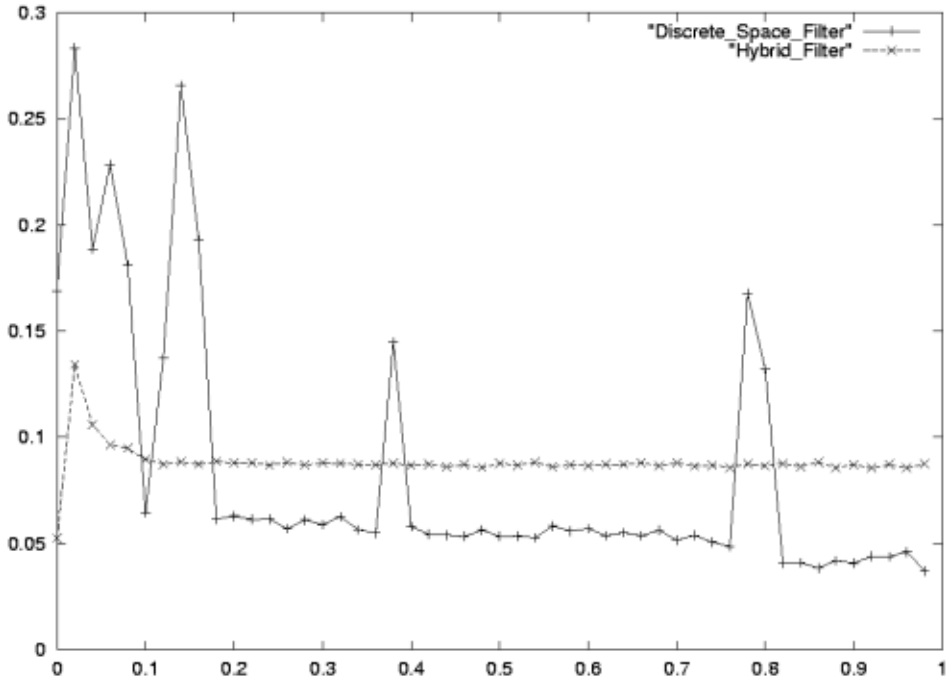

Figure 4. Average mean computation time for Scenario A.

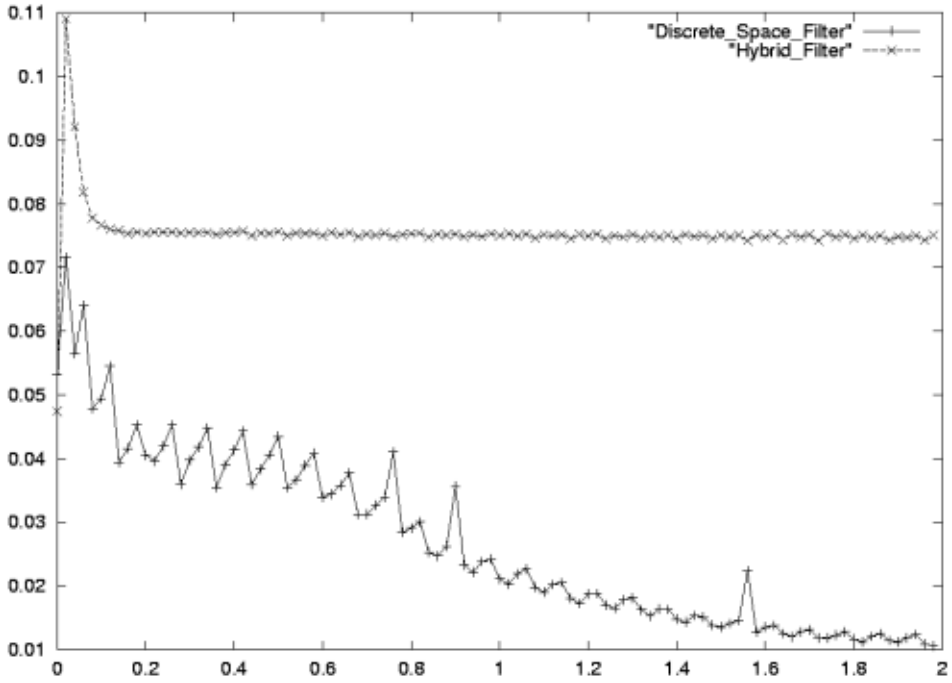

Figure 5. Average mean computation time for Scenario B.

5. CONCLUSIONS

For both simulated scenarios, the refining hybrid method exhibits superior performance in fidelity. Although this method required greater computation time then the discrete space filter in our tests, the requirement for the acoustic predicting problem is real-time performance, and this can be met using modern computers, under conditions similar to those in our simulations (see Sect. (4.2)). Improvements in speed can be achieved with the hybrid filter, by reducing the starting number of particles, with little loss in accuracy, because the observations in this problem are relatively accurate. Our simulated discrete space filter's crude grid is not sufficient to compete against the hybrid's continuous space particles when very accurate predictions are needed. As a future goal, the discrete space method's implementation should be improved to accommodate dynamically refining the grid partition N in high dimensions with little additional computational costs. For now, the discrete space filter will fully accommodate fast, relatively low fidelity tracking and prediction. APR's applications demand high fidelity predictions in real-time, and for this we choose the hybrid method over the discrete space method.

ACKNOWLEDGMENTS

The authors gratefully acknowledge the support and sponsorship of Acoustic Positioning Research Inc., Lockheed Martin Naval Electronics and Surveillance Systems, Lockheed Martin Canada, the Pacific Institute for the Mathematical Sciences, the Natural Science and Engineering Research Council (NSERC) through the Prediction in Interacting Systems (PINTS) centre of the Mathematics of Information Technology and Complex Systems (MITACS) network of centres of excellence, and the University of Alberta.

REFERENCES

1. D. Ballantyne, H. Chan, and M. Kouritzin, "A novel branching particle method for tracking," *Proceedings of SPIE, Signal and Data Processing of Small Targets 2000* **4048**, pp. 277–287, 2000.

2. P. Del Moral and G. Salut, "Non-linear filtering using Monte Carlo particle methods," *C.R. Acad. Sci. Paris* **320, Série I**, pp. 1147–1152, 1995.
3. P. Del Moral, M. Kouritzin, and L. Miclo, "On a class of discrete generation interacting particle systems," *Electronic Journal of Probability* **paper No. 16**, pp. 1–20, 2001.
4. M. A. Kouritzin, H. Long and W. Sun, Markov chain approximations to nonlinear filtering equations for reflecting diffusion processes. Preprint, 2001.
5. D. Ballantyne, M. Kouritzin, H. Long, and W. Sun, "Discrete-Space Particle Filters for Reflecting Diffusions," *2002 IEEE Aerospace Conference Proceedings* **4048**, pp. 277–287, 2002.